Selective Transporting of Lithium Ion by Shape Selective Molecular Sieves ZSM-5 in PEO-Based Composite Polymer Electrolyte

Jingyu Xi,[†] Shaojun Miao,[‡] and Xiaozhen Tang*,[†]

School of Chemistry and Chemical Technology, Shanghai Jiao Tong University, Shanghai 200240, China, and State Key Laboratory of Catalysis, Dalian Institute of Chemical Physics, Chinese Academy of Sciences, Dalian 116023, China

Received June 11, 2004; Revised Manuscript Received July 24, 2004

ABSTRACT: To elucidate the mechanism of the enhancement of lithium ion transference numbers, T_{Li^+}, induced by ZSM-5 in PEO-based composite polymer electrolyte, different types of other fillers, such as ceramic fillers (SiO_2 and Al_2O_3), solid superacid (SO_4^{2-}/ZrO_2), layered materials (montmorillonite), and mesoporous materials (MCM-41, HMS, and SBA-15), are selected to compare with ZSM-5 molecular sieves. The experimental results suggest that ZSM-5 may enhance the T_{Li^+} of PEO-based composite polymer electrolytes in three ways: (1) Lewis acid−base interactions, resulting in the release of more "free" Li^+ cations; (2) selective passing of Li^+ cations due to the special pore size of ZSM-5 and electrostatic repulsion for ClO_4^- anions due to the negative environment in the channels of ZSM-5; (3) the cation-exchange centers in the framework of ZSM-5, suggesting that the Li^+ cation can be ion-exchanged into the channels for charge balance, namely, provide a special conducting pathway for Li^+ cation. In addition, room temperature ionic conductivity of the composite polymer electrolyte can also be increased by about 2 orders of magnitude. The high lithium ion transference numbers combined with a suitable ionic conductivity of PEO−$LiClO_4$−ZSM5 composite polymer electrolyte suggest that it can be used as candidate electrolyte material for all solid-state rechargeable lithium polymer batteries.

Introduction

All solid-state lithium polymer batteries (LPBs) may be one of the best choices for electrochemical power source of the future characterized by its high energy densities, good cyclability, reliability, and safety.[1,2] PEO−LiX (X = ClO_4^-, I^-, BF_4^-, PF_6^-, $CF_3SO_3^-$, etc.)-based polymer electrolytes have received extensive attention[3,4] due to its potential capability to be used as candidate material instead of traditional liquid electrolytes, since Wright et al. found that the complex of PEO and alkaline salts had the ability of ionic conductivity in 1973.[5] The lithium ion transference number, T_{Li^+}, is one of the most important parameters for rechargeable lithium ion batteries. A relative high T_{Li^+} can eliminate the concentration gradients within the battery and can ensure the battery operation under high current density.[1,3] Unfortunately, Li^+ cations in PEO−LiX-based polymer electrolytes can coordination not only with the ether O in PEO chains but also with the O atoms in ClO_4^-, and then its transport ability is restricted, resulting in a very low T_{Li^+} value (<0.2).[3] Two different strategies have been used to enhance the T_{Li^+} of the polymer electrolytes: (1) By the addition of ceramic fillers, such as SiO_2 and Al_2O_3, into the PEO−$LiClO_4$ system, T_{Li^+} of the resulting composite polymer electrolytes (CPE) can be increased because the Lewis acid sites on the surface of these fillers can interact with the O atoms in PEO and/or ClO_4^- (Lewis base) and hence weaken the interactions between these O atoms and Li^+ and then release more "free" Li^+ to improve the T_{Li^+}.[3,6] (2) Synthesis of single ionic conductor-based polymer electrolytes, in which case the counteranions are fixed.[7]

The wide use of microporous molecular sieves ZSM-5 in the fields such as selective adsorption and separation and shape selective catalysis, due to its special pore size and two-dimensional interconnect channels,[8,9] inspired us to evaluate whether such a selective effect can be applied to select passing different charge carriers in PEO-based composite polymer electrolyte by using ZSM-5 as the filler. Furthermore, the cation-exchange centers resulting from the periodic replacement of $[AlO_4]^-$ for $[SiO_4]$ in the framework of ZSM-5 shows that Li^+ cation can be ion-exchanged into the well-defined channels for charge balance, which may provide another contribution for the enhancement of lithium ion transference numbers. In previous work, we have found that ZSM-5 can enhance the electrochemical properties such as ionic conductivity, lithium ion transference numbers, lithium electrode interface stability, and electrochemical stability window at the same time.[10]

To elucidate the mechanism of the enhancement of T_{Li^+} induced by ZSM-5 in PEO-based polymer electrolyte, different types of other fillers, such as ceramic fillers (SiO_2 and Al_2O_3), solid superacid (SO_4^{2-}/ZrO_2), layered materials (montmorillonite), and mesoporous materials (MCM-41, HMS, and SBA-15), are selected to compare with ZSM-5 molecular sieves; the experiment results are presented and discussed in this paper. In addition, the effects of Si/Al ratio of ZSM-5 and the content of ZSM-5 on the T_{Li^+} of the PEO-based polymer electrolyte are also studied.

Experimental Section

Preparation of Mesoporous Silica. MCM-41 was synthesized in classical alkaline media using conventional literature recipes.[11] Typically, solid cetyltrimethylammonium bromide (CTMABr) is dissolved in NaOH solution, to which a tetramethyl orthosilicate (TMOS) solution is then added. The final pH, stabilized to about 12.5, was decreased and adjusted at 10.5 by slowly adding a diluted HNO_3 solution. The

[†] Shanghai Jiao Tong University.
[‡] Chinese Academy of Sciences.
* Corresponding author: Tel 86-21-54747142; Fax 86-21-54743264; e-mail xtang@sjtu.edu.cn.

10.1021/ma048849d CCC: $27.50 © 2004 American Chemical Society
Published on Web 10/19/2004

precipitate is homogenized by vigorous stirring for 1 h at ambient temperature and then heated at 383 K in a Teflon-coated stainless steel autoclave for 24 h under autogenous pressure. The white precipitate was filtered, washed with cold water, and dried at 353 K overnight and finally calcined at 873 K for 4 h.

HMS was synthesized at ambient conditions by adopting the approach reported elsewhere[12] using dodecylamine and tetraethyl orthosilicate (TEOS) as a neutral template and silica precursor, respectively. Thus, the obtained sample was filtered, washed with warm distilled water, dried at 383 K, and finally calcined at 813 K in air for 6 h.

SBA-15 was synthesized by using the triblock copolymer Pluronic P123 ($EO_{20}PO_{70}EO_{20}$, M_{av} = 5800, BASF) as a surfactant and tetraethoxylsilicon (TEOS) as a silica source.[13] In a typical synthesis experiment, TEOS (20.8 g) was added to a mixture of P123 (10 g), HCl (62.57 g, 35 wt %), and deionized water (319 g) under static conditions at 312 K. After the mixture was stirred for 24 h, the mesostructured products thus formed were cured at 373 K for an additional 24 h. The products were filtered, dried without washing, and calcined at 823 K for 5 h.

Preparation of Solid Superacid SO_4^{2-}/ZrO_2. The zirconia support was prepared by hydrolysis of zirconium oxychloride with ammonia, as already described.[14] The precipitate zirconium hydroxide was washed with deionized water until no ammonia and chloride ions were detected in the washings, the absence of which was confirmed through the phenolphthalein and silver nitrate tests, respectively. The white precipitate zirconium hydroxide was then dried in an oven at 383 K for 24 h. Sulfation of this hydrous zirconia was done by percolating 1 mol L^{-1} H_2SO_4 solution through it. The sulfated zirconium hydroxide was then calcined in air at 923 K for 3 h to obtain the final SO_4^{2-}/ZrO_2.

About 25 mg of sample was shaken with 1 mL of a solution of Hammett indicator diluted in 10 mL of cyclohexane and left to equilibrate for 2 h. The color of the sample was then noted. The acid strength is quoted as being stronger than the weakest indicator which exhibits a color change but weaker than the strongest base that produces no change. The Hammet acidity function H_0 of as-prepared SO_4^{2-}/ZrO_2 is −16.0, confirming the successful preparation of this solid superacid.

Other Materials. SiO_2 (10 nm) and Al_2O_3 (60 nm) (Zhoushan Nano Co. Ltd., China) were vacuum-dried for 24 h at 200 °C prior to use. LiMMT was obtained by the ion exchange method from NaMMT (CEC = 100 mmol/100 g, obtained from Inst. Chem. CAS) and denoted as MMT. Li−ZSM-5 was obtained by the ion exchange method from H−ZSM-5 (SiO_2/Al_2O_3 = 25, 38, and 50, obtained from Nankai University Catalyst Co.) and denoted as ZSM-5. TS-1 molecular sieves was obtained from BASF (Si/Ti = 64).

Poly(ethylene oxide), PEO, M_w = 1 000 000 (Shanghai Liansheng Chem. Tech. Co. Ltd.), and $LiClO_4$, A.R. (Shanghai Second Regent Co.), were vacuum-dried for 24 h at 50 and 120 °C, respectively, before use. Acetonitrile, A.R. (Shanghai Chemical Regent Co.), was dehydrated by 4A molecular sieves before use.

Preparation of Composite Polymer Electrolytes. The preparation of composite polymer electrolyte films involved first the dispersion of the PEO and $LiClO_4$ in anhydrous acetonitrile, followed by the addition of the filler. The resulting slurry was cast on to a Teflon plate, and then the plate was placed into a self-designed equipment, under the sweep of dry air with a flow rate of 10 L min^{-1}, to let the solvent slowly evaporate. Finally, the result films were dried under vacuum at 50 °C for 24 h to get rid of the residue solvent. These procedures yielded translucent homogeneous self-supporting films of thickness ranging from 100 to 200 μm (Figure 1). All the CPE films were stored in an argon atmosphere glovebox before testing. The composite polymer electrolyte samples used in this study were denoted as PEO_{10}−$LiClO_4$-*X*% filler, in which the EO/Li ratio was fixed at 10 for all samples and the content of filler, *X*, ranged from 0 to 30 wt % of the PEO weight.

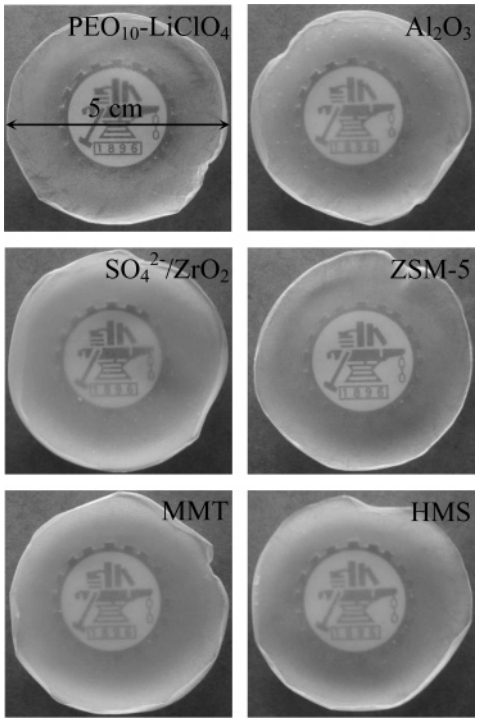

Figure 1. Photos of PEO_{10}−$LiClO_4$ and PEO_{10}−$LiClO_4$−10% filler composite polymer electrolytes recorded with a digital camera.

N_2 Adsorption−Desorption Measurement. Nitrogen adsorption isotherms were measured with an ASAP2010 adsorption analyzer (Micromeritics) at liquid nitrogen temperature. Prior to the measurements, all samples were degassed at a temperature of 250 °C for at least 3 h. The specific surface area was calculated from the adsorption data in the relative pressure interval from 0.04 to 0.2 using the Brunauer−Emmett−Teller (BET) method. Pore sizes and pore size distribution curves were calculated by the BJH method from the desorption branch. The total pore volume was estimated from the amount adsorbed at a relative pressure of 0.99.

XRD Measurement. X-ray diffraction (XRD) patterns were recorded by using a Bruker D8 Advance instrument equipped with Cu Kα radiation performed at 40 kV and 40 mA. A scan rate of 1.0° min^{-1} over the range of 0.5−10° (2θ) was used for detecting the characteristic diffraction of MMT and mesoporous silica MCM-41, HMS, and SBA-15.

FT-IR Measurement. Infrared spectra were recorded on a PE PARAGN1000 instrument with a wavenumber resolution of 2 cm^{-1} in the frequency range of 4000−400 cm^{-1}. For that measurement, the mixed slurry were cast on a KBr wafer and dried via the same steps used in the preparation of composite polymer electrolyte films.

Ionic Conductivity. Ionic conductivity of the composite polymer electrolytes was determined by ac impedance spectroscopy. The electrolyte was sandwiched between two stainless steel (SS) blocking electrodes to form a symmetrical SS/electrolyte/SS cell. The cell was placed into a self-designed oven coupled with a temperature controller. For each temperature, at least 30 min was allowed before the impedance response was recorded. The impedance tests were carried out in the 1 MHz−1 Hz frequency range using a Solartron 1260 impedance/gain-phase analyzer coupled with a Solartron 1287 electrochemical interface.

Lithium Ion Transference Numbers. The lithium ion transference number, T_{Li^+}, was evaluated using the method originally proposed by Vincent and Bruce.[15] The method consists of initial measurement of the lithium interfacial resistance (R_0) by impedance spectroscopy in the 100 kHz−0.1 Hz frequency range, application of a small voltage (<10 mV) until a steady current was obtained (I_{ss}), and finally measurement of the interfacial resistance (R_f) by impedance

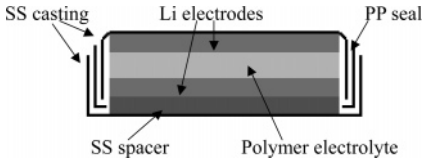

Figure 2. Schematic design of coin cell used for lithium ion transference number measurements. SS = stainless steel; PP = polypropylene.

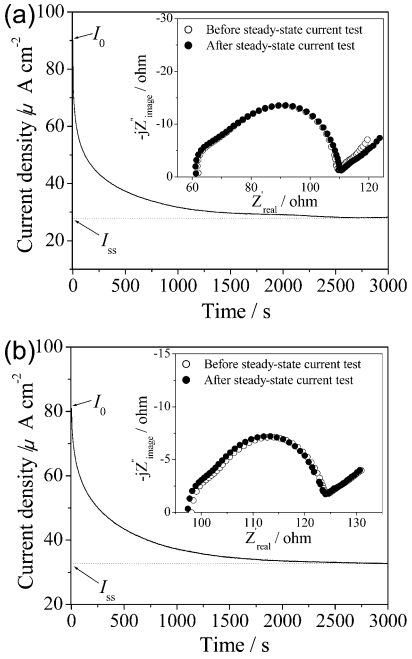

Figure 3. Current response of Li/PEO_{10}−$LiClO_4$/Li cell (a) and Li/PEO_{10}−$LiClO_4$−10% ZSM5/Li cell (b) under a dc voltage as a function of time at 70 °C. The inset shows the initial and steady-state impedance response of the cell.

spectroscopy in the 100 kHz−0.1 Hz frequency range. T_{Li^+} was calculated using the following equation:

$$T_{Li^+} = \frac{I_{ss}}{I_0}\left(\frac{\Delta V - I_0 R_0}{\Delta V - I_{ss} R_f}\right)$$

where I_0 was the initial current and was calculated from the voltage and the overall cell resistance by

$$I_0 = \frac{\Delta V}{R_b + R_0}$$

where R_b was the bulk resistance of the composite polymer electrolyte. Measurements were performed using a Solartron 1260 impedance/gain-phase analyzer coupled with a Solartron 1287 electrochemical interface. The electrolyte was sandwiched between two lithium-unblocking electrodes to form a symmetrical Li/electrolyte/Li cell used for a T_{Li^+} test, and the schematic design of the coin cell (CR2025) is given in Figure 2. The cell was assembled and sealed in an argon-filled UNILAB glovebox (O_2 < 0.1 ppm; H_2O < 0.1 ppm).

Results and Discussion

T_{Li^+} of the polymer electrolyte was evaluated using steady-state current technique proposed by Bruce et al.[15] Experimental results of the pristine PEO_{10}−$LiClO_4$ and PEO_{10}−$LiClO_4$−10% ZSM5 composite polymer electrolyte are shown in Figure 3 as examples. All parameters used for the calculation of T_{Li^+} can be obtained directly from the impedance response and current response of the Li/electrolyte/Li cell, as shown in Figure 3. T_{Li^+} values of PEO_{10}−$LiClO_4$ and PEO_{10}−$LiClO_4$−10% filler composite polymer electrolytes are summarized in Table 1.

It is obvious that the T_{Li^+} value can be increased in different degrees by the addition of all inorganic fillers. In the case of pristine PEO−$LiClO_4$, Li^+ cations can complex not only with the ether O in PEO chains but also with the O atoms in ClO_4^-, and then its transport ability is restricted, resulting in a very low T_{Li^+} value (<0.2) of PEO−$LiClO_4$ electrolyte,[3,6] consistent with our results in Table 1. After the addition of traditional ceramic fillers (or nanooxides), such as SiO_2 and Al_2O_3, T_{Li^+} can be increased slightly through the well-known Lewis acid−base interactions.[3] The Lewis acid sites on the surface of SiO_2 and Al_2O_3 can interact with O atoms in PEO chains and ClO_4^- anions (Lewis base) and hence weaken the interactions between these O atoms and Li^+ cations. As a result, more "free" Li^+ cations are released, and of course the value of T_{Li^+} is enhanced, as shown in Table 1.

To prove the above Lewis acid−base interactions exist in the composite polymer electrolytes, we selected SO_4^{2-}/ZrO_2, a well-known solid superacid[14] whose Lewis acidity (Hammet acidity function, $H_0 = -16.0$) is much stronger than that of SiO_2 and Al_2O_3, as the filler, and the above Lewis acid−base interactions between the filler and PEO chains and/or ClO_4^- anions should make the promotion effect of SO_4^{2-}/ZrO_2 be better than SiO_2 and Al_2O_3. The experiments results listed in Table 1 show that the T_{Li^+} enhancement decreases in the order SO_4^{2-}/ZrO_2 > Al_2O_3 > SiO_2, consistent with the theoretical hypothesis.

In the case of ZSM-5 molecular sieves, T_{Li^+} of composite polymer electrolyte can of course be enhanced by the same Lewis acid−base interactions, but an even more important fact is that ZSM-5, as one kind of microporous molecular sieve, has two-dimensional open channels which are interconnected to each other. The pore sizes of ZSM-5 are 0.53 nm × 0.56 nm for straight channel and 0.51 nm × 0.55 nm for Z type channel, as shown in Figure 4. On the other hand, the ionic diameters of Li^+ cation and ClO_4^- anion are 0.152 and 0.474 nm, respectively, and as a result, Li^+ can enter and path through the channels of ZSM-5 more easily than ClO_4^-; in other words, ZSM-5 has a selective action on the transporting of different charge carriers, which is beneficial for enhancing the T_{Li^+} of the composite polymer electrolyte. In addition, the negative charge environment in the channels of ZSM-5 is in favor of the entrance of cations Li^+; on the contrary, it is hard for the anion ClO_4^- to enter the channels of ZSM-5 due to the electrostatic repulsion. The composite polymer electrolyte doped with ZSM-5 has the highest T_{Li^+} (see Table 1) proves the above hypothesis.

TS-1 molecular sieves are usually synthesized by replacing parts of [SiO_4] with [TiO_4] in the framework of ZSM-5.[16] Although TS-1 has the same pore sizes and channel structure like ZSM-5, its Lewis acidity on the framework is stronger than that of ZSM-5 due to the existence of Ti in the framework. However, the channels of TS-1 do not have cation-exchange centers due to the charge-balancing comparison with ZSM-5. As a result, the enhancement of T_{Li^+} of the composite polymer electrolyte induced by TS-1 molecular sieves may be attributed to two reasons: (1) Lewis acid interactions between the Lewis acid sites on the framework of TS-1 and PEO chains and/or ClO_4^- anions, like the case of

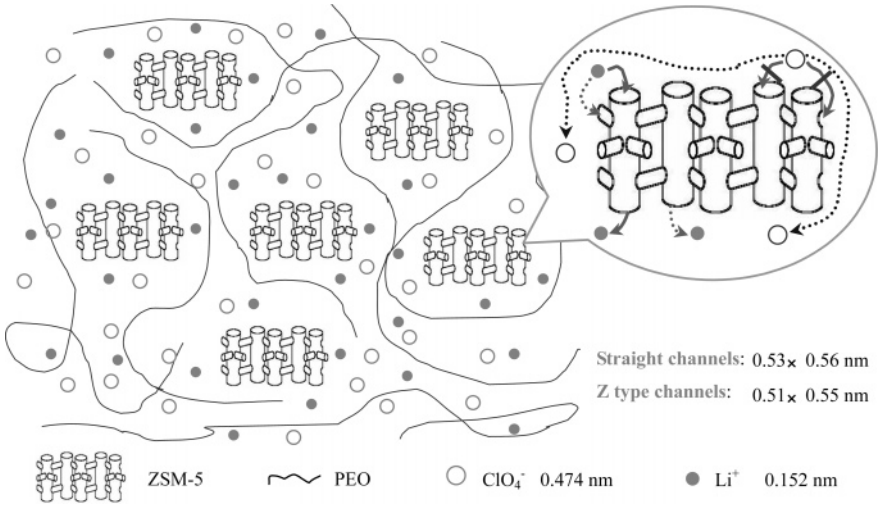

Figure 4. Schematic representation of selective passing of Li^+ cation by ZSM-5 in PEO−$LiClO_4$−ZSM5 composite polymer electrolyte.

Table 1. Lithium Ion Transference Numbers of PEO_{10}−$LiClO_4$ and PEO_{10}−$LiClO_4$−10% Filler Composite Polymer Electrolytes

filler type		av size, nm[a]	surface area, $m^2\,g^{-1}$ [b]	pore size or interlayer spacing, nm	T_{Li^+}[c]
filler free					0.19
nanooxide	SiO_2	10	600		0.24
	Al_2O_3	60	180		0.25
solid superacid	SO_4^{2-}/ZrO_2	60−70	110		0.29
microporous molecular sieves	ZSM-5[d]	500	300	0.51 × 0.55 [10-ring channel 100] 0.53 × 0.56 [10-ring channel 010]	0.35
	TS-1	500	200	0.51 × 0.55 [10-ring channel 100] 0.53 × 0.56 [10-ring channel 010]	0.31
layered material	MMT	∼1000	150	1.78[e]	0.25
mesoporous material	MCM-41	200	650	3.42[f]	0.24
	HMS	200	670	4.37[f]	0.24
	SBA-15	500	600	5.80[f]	0.23

[a] Evaluated from SEM images. [b] Obtained from BET results. [c] Evaluated from Li/polymer electrolyte/Li cells at 70 °C. All tests were repeated at least three times, and the values of T_{Li^+} were reproducible within 0.01. All cells were stored under open-circuit conditions at 70 °C for at least 72 h before each test. [d] $SiO_2/Al_2O_3 = 25$. [e] Calculated from the diffraction data. [f] Obtained from N_2 adsorption−desorption results.

SiO_2 and Al_2O_3; (2) selective passing of charge carriers based on their size induced by the special pore size of TS-1, like the case of ZSM-5. Experimental results in Table 1 show that T_{Li^+} of composite polymer electrolyte doped with TS-1 (0.31) is higher than that of SiO_2 (0.24), Al_2O_3 (0.25), and SO_4^{2-}/ZrO_2 (0.29) but lower than that of ZSM-5 (0.35) are consistent with above discussion.

To further confirm the selective passing effect of charge carriers induced by the special pore size and channels of ZSM-5, we selected layered montmorillonite (MMT) and some ordered mesoporous silica, MCM-41, HMS, and SBA-15 as fillers, whose layer distance and/or pore size are large enough compared with all charge carriers in the composite polymer electrolyte. Figure 5 shows the X-ray diffraction patterns of these fillers and composite polymer electrolytes based on these fillers. The diffraction peaks corresponding to the mesoporous silica become weaker when doping in the PEO_{10}−$LiClO_4$ electrolyte due to the dilution reason; however, the peak positions do not change, suggesting that all mesoporous silica can maintain their pore size and pore structures effectively under the intercalation of PEO chains (Figure 5b−d). However, the interlayer spacing of MMT increases from 1.50 to 1.78 nm after the intercalation of PEO chains (Figure 5a).[17] The T_{Li^+} value of MMT-based composite polymer electrolyte is 0.25, which is close to the case of SiO_2 and Al_2O_3. All three mesoporous silica have two-dimensional hexagonal pore structures with

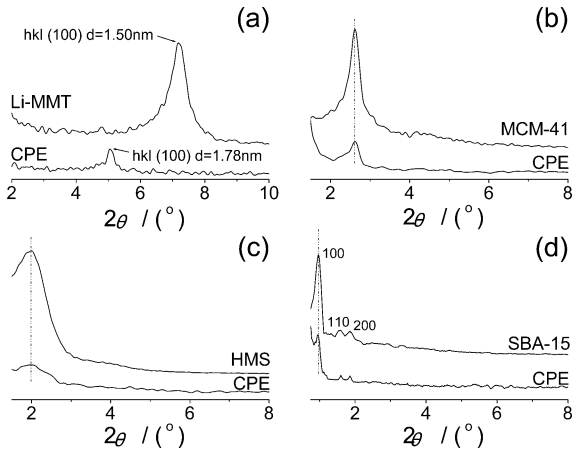

Figure 5. Low-angle X-ray diffraction patterns of the fillers and corresponding composite polymer electrolytes: (a) MMT, (b) MCM-41, (c) HMS, and (d) SBA-15.

the pore size in the range of 3−6 nm (see Table 1), and the composite polymer electrolytes based on these mesoporous silica fillers also show the T_{Li^+} values close to the case of SiO_2. T_{Li^+} decreases with the increases of pore size or interlayer spacing, strongly suggesting that porous and/or layered fillers have no selective passing effect on the transporting of different ions when the pore size or interlayer spacing of these fillers are too large comparing with both Li^+ cation and ClO_4^- anion. The

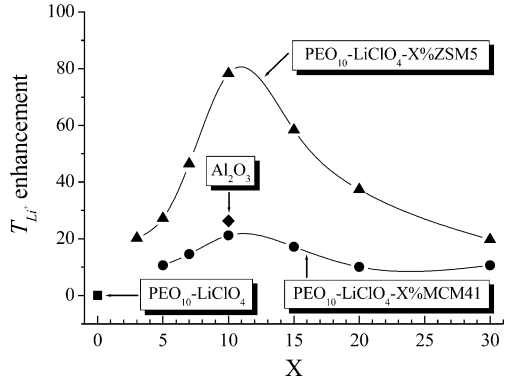

Figure 6. Effect of filler content on the enhancement of lithium-ion transference number of PEO_{10}−$LiClO_4$−*X*% filler composite polymer electrolytes at 70 °C.

slight enhancement of T_{Li^+} in these cases should only be attributed to the Lewis acid−base interaction mentioned above.

The effects of filler content on the enhancement of T_{Li^+} of PEO_{10}−$LiClO_4$−*X*% ZSM5 (SiO_2/Al_2O_3 = 25) and PEO_{10}−$LiClO_4$−*X*% MCM41 composite polymer electrolytes compared with pristine PEO_{10}−$LiClO_4$ are shown in Figure 6. For PEO_{10}−$LiClO_4$−*X*% MCM41, T_{Li^+} first increases with MCM-41 content and reaches a maximum value of 0.24, about 20% percentage higher than that of pristine PEO_{10}−$LiClO_4$, when $X = 10$. This can be explained by the fact that more MCM-41 fillers can provide more Lewis acid sites, which can interact with the ether O in PEO chains and release more "free" Li^+. And as a result, T_{Li^+} increases with MCM-41 content. However, T_{Li^+} decreases when the MCM-41 content further increases, which can be attributed to the aggregation of MCM-41 filler at high loading content. The aggregation of MCM-41 results in the decreases of the effective interface area between PEO and MCM-41, and hence, the Lewis acid−base interaction between MCM-41 and PEO decreases.

The effect of ZSM-5 content on T_{Li^+} of PEO_{10}−$LiClO_4$−*X*% ZSM5 shows the same trend like PEO_{10}−$LiClO_4$−*X*% MCM41; however, T_{Li^+} of PEO_{10}−$LiClO_4$−*X*% ZSM5 is higher than that of PEO_{10}−$LiClO_4$−*X*% MCM41 in all filler contents. Figure 4 shows a schematic illustration of the mechanism of the selective passing of Li^+ cations induced by the ZSM-5 in PEO−$LiClO_4$−ZSM5 composite polymer electrolyte. It is plausible to propose that this selective passing effect can really work only when there are enough ZSM-5 particles highly dispersed in the composite polymer electrolyte. In this case, ZSM-5 particles are separated and/or surrounded by PEO chains, and the distance between each ZSM-5 particle is very small. The relatively small Li^+ cations can transport in the composite polymer electrolyte either coupled with the segment movement of PEO chains or direct passing through the channels of ZSM-5 under the electric field; however, the ClO_4^- anions are difficult to pass through the channels of ZSM-5 due to their relatively large size, and electrostatic repulsion of the negative environment in the channels of ZSM-5 and ClO_4^- anions can only transport through the free volume of the composite polymer electrolyte. It can be seen from Figure 6 that T_{Li^+} of PEO_{10}−$LiClO_4$−*X*% ZSM5 increases sharply with ZSM-5 content and reaches a maximum value of about 0.35, about 80% percentage higher than that of pristine PEO_{10}−$LiClO_4$ and 3 times higher compared with the enhancement

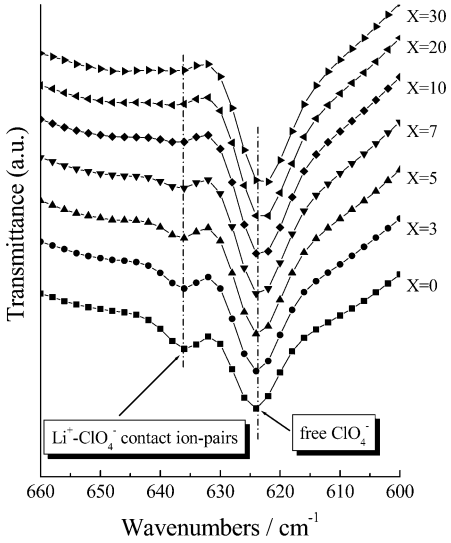

Figure 7. FT-IR spectra in the wavenumber range of 600−660 cm^{-1} of PEO_{10}−$LiClO_4$ and PEO_{10}−$LiClO_4$−*X*% ZSM5 composite polymer electrolytes.

induced by the same content of MCM-41 filler, when $X = 10$. This result is consistent with above discussion. When the content of ZSM-5 further increases, T_{Li^+} decreases and maintains a value of about 0.23−0.24. This can be explained by the aggregation of ZSM-5 particles at high loading content, which results in the blocking of the pores and/or channels of ZSM-5. In this case, ZSM-5 may act as silica filler without pores, and the slightly enhancement of T_{Li^+}+ can be attributed to the Lewis acid−base interaction like the case of SiO_2 and mesoporous silica MCM-41.

The FT-IR peak of $\upsilon(ClO_4^-)$ band at the region of 660−600 cm^{-1} is frequently used to analyze ion−ion interactions in PEO−$LiClO_4$-based polymer electrolytes.[18] In the PEO_{10}−$LiClO_4$ case (Figure 7), the peak of $\upsilon(ClO_4^-)$ band splits into two peaks at ∼624 and ∼635 cm^{-1}, demonstrating that at least two different kinds of ClO_4^- anions exist in this complex. Salomon et al. suggest that the $\upsilon(ClO_4^-)$ band centered between 630 and 635 cm^{-1} is associated with the presence of Li^+−ClO_4^- contact-ion pairs whereas the band centered at about 623 cm^{-1} can be attributed to free ClO_4^- anions.[18] As can be seen from Figure 7, the peak characteristic for "free" ClO_4^- is much larger than that of contact-ion pairs. This is because that the relatively low content of $LiClO_4$ (EO/Li = 10) is helpful for its dissolving in the PEO matrix.

For composite polymer electrolytes containing ZSM-5, the peak characteristic of contact-ion pairs at ∼635 cm^{-1} becomes more smaller, and only a trace shoulder peak corresponds to contact-ion pairs can be detected when the content of ZSM-5 reaches 10 wt % of PEO weight, suggesting that the ratio of free Li^+ increases with ZSM-5 content, which can be attributed to the Lewis acid−base interactions between the Lewis acid sites on the framework of ZSM-5 and ether O in PEO chains and O atoms in ClO_4^- anions, consistent with the result in Figure 6 that T_{Li^+} of PEO_{10}−$LiClO_4$−*X*% ZSM5 increases with the content of ZSM-5.

FT-IR spectra of the composite polymer electrolytes PEO_{10}−$LiClO_4$−10% filler doped with different fillers are compared in Figure 8. It is obvious that the composite polymer electrolyte doped with ZSM-5 has the lowest ratio of Li^+−ClO_4^- contact-ion pairs compared

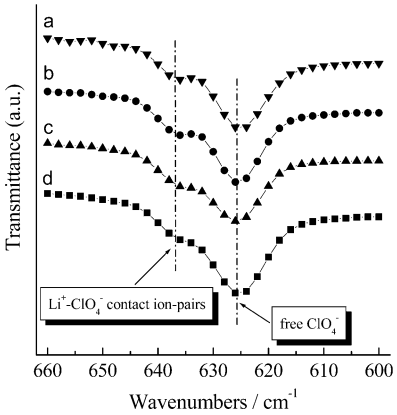

Figure 8. FT-IR spectra in the wavenumber range of 600−660 cm^{-1} of PEO_{10}−$LiClO_4$−10% filler composite polymer electrolytes: (a) SiO_2, (b) Al_2O_3, (c) SO_4^{2-}/ZrO_2, and (d) ZSM-5.

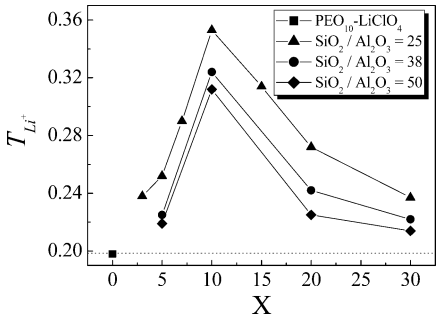

Figure 9. Effect of SiO_2/Al_2O_3 ratio of ZSM-5 and the content of ZSM-5 on lithium ion transference numbers of PEO_{10}−$LiClO_4$−*X*% ZSM5 composite polymer electrolytes at 70 °C.

with other samples, which is in agreement with the results in Table 1.

On the basis of the above results and discussions, it can be concluded that ZSM-5 helps to increase the T_{Li^+} of PEO_{10}−$LiClO_4$−*X*% ZSM5 composite polymer electrolytes through at least two ways, namely, Lewis acid−base interactions (attributed to the Lewis acid sites on the framework of ZSM-5) and selective passing of charge carriers (attributed to the special pore size and channel structures of ZSM-5). In view of that the negative environment in the channels of ZSM-5 may provide conducting pathway for Li^+ cations, three ZSM-5 with different SiO_2/Al_2O_3 ratio (25, 38, and 50) are selected to further study whether the cation exchange capability of ZSM-5 has any effect on the T_{Li^+} of PEO_{10}−$LiClO_4$−*X*% ZSM5 composite polymer electrolytes, and the experiment results are shown in Figure 9.

The cation-exchange centers resulting from the periodic replacement of $[AlO_4]^-$ for $[SiO_4]$ in the framework of ZSM-5 means that the cation-exchange capability of ZSM-5 increases with the decreases of SiO_2/Al_2O_3 ratio in its framework. It can be seen from Figure 9 that the effect of ZSM-5 content on the T_{Li^+} value of the PEO_{10}−$LiClO_4$−*X*% ZSM5 composite polymer electrolytes show the same trend for all SiO_2/Al_2O_3 ratios that T_{Li^+} first increases sharply with the increase of ZSM-5 content and reaches a maximum value when the content of ZSM-5 up to 10 wt % of PEO weight and then decreases when the ZSM-5 content further increases. However, it should be noted that T_{Li^+} increases slightly with cation-exchange capability of ZSM-5 in all loading content, suggesting that the Li^+ cation can pass through the well-defined channels of ZSM-5 for charge balance, which provides another contribution for the enhancement of T_{Li^+}.

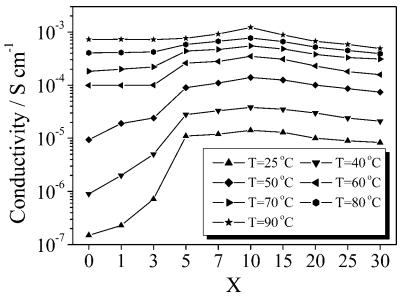

Figure 10. Effect of ZSM-5 ($SiO_2/Al_2O_3 = 25$) content on ionic conductivity of the composite polymer electrolytes PEO_{10}−$LiClO_4$−*X*% ZSM5 at different temperatures.

In previous work, we have found that ZSM-5 can obviously increase the ionic conductivity of PEO-based electrolyte.[10] Figure 10 shows the effect of ZSM-5 content on the ionic conductivity of PEO_{10}−$LiClO_4$−*X*% ZSM5 at different temperatures. Ionic conductivity first increases with ZSM-5 content and reaches a maximum value, which is nearly 100 times higher than the pristine PEO_{10}−$LiClO_4$ (at 25 °C), by 10% loading content. When ZSM-5 content increases further, ionic conductivity decreased. The existence of the maximum value of ionic conductivity indicates that there are two opposing effects of ZSM-5 on ionic conductivity of PEO_{10}−$LiClO_4$−*X*% ZSM5. The active effect induces by ZSM-5, as mentioned above, can increase the ionic conductivity of the composite polymer electrolyte. On the other hand, when the content of ZSM-5 is too high, the blocking effect on the transporting of charge carriers resulting from the aggregating of the ZSM-5 may decrease the ionic conductivity of the composite polymer electrolyte.

Conclusions

The present results reveal that microporous molecular sieves ZSM-5 may enhance the lithium ion transference numbers of the PEO-based composite polymer electrolyte through three ways: (1) Lewis acid−base interaction between the Lewis acid sites on the framework of ZSM-5 and ether O in PEO chains and O atoms in ClO_4^- anions, resulting in the release of more "free" Li^+ cations; (2) selective passing of Li^+ cations due to the special pore size and channel structures of ZSM-5 and electrostatic repulsion for ClO_4^- anions due to the negative environment in the channels of ZSM-5; (3) the cation-exchange centers resulting from the periodic replacement of $[AlO_4]^-$ for $[SiO_4]$ in the framework of ZSM-5 means that Li^+ cation can be ion-exchanged into the well-defined channels for charge balance and provide the other contribution for the enhance of lithium ion transference numbers. The high lithium ion transference numbers of PEO−$LiClO_4$−ZSM5 composite polymer electrolyte suggest that it can be used as candidate electrolyte material for all solid-state rechargeable lithium polymer batteries.

Acknowledgment. This work was supported by the Key Science and Technology Project of Shanghai (Grant 02dz11002).

References and Notes

(1) Tarascon, J. M.; Armand, M. *Nature (London)* **2001**, *414*, 359.
(2) (a) Scrosati, B.; Croce, F.; Panero, S. *J. Power Sources* **2001**, *100*, 93. (b) Murata, K.; Izuchi, S.; Yoshihisa, Y. *Electrochim. Acta* **2000**, *45*, 1501. (c) Scrosati, B. *Chem. Rec.* **2001**, *1*, 173.

(3) Croce, F.; Appetecchi, G. B.; Persi, L.; Scrosati, B. *Nature (London)* **1998**, *394*, 456.
(4) (a) Meyer, W. H. *Adv. Mater.* **1998**, *10*, 439. (b) Jacob, M. M. E.; Hackett, E.; Giannelis, E. P. *J. Mater. Chem.* **2003**, *13*, 1. (c) Chandrasekhar, V. *Adv. Polym. Sci.* **1998**, *135*, 139. (d) Gray, F. M. *Polymer Electrolytes*; Royal Society of Chemistry: Cambridge, 1997. (e) Gray, F. M. *Solid Polymer Electrolytes: Fundamentals and Technological Applications*; VCH: New York, 1991. (f) Gadjourova, Z.; Andreev, Y. G.; Tunstall, D. P.; Bruce, P. G. *Nature (London)* **2001**, *412*, 520. (g) Stoeva, Z.; Litas, I. M.; Staunton, E.; Andreev, Y. G.; Bruce, P. G. *J. Am. Chem. Soc.* **2003**, *125*, 4619.
(5) (a) Fenton, D. E.; Parker, J. M.; Wright, P. V. *Polymer* **1973**, *14*, 589. (b) Wright, P. V. *Br. Polym. J.* **1975**, *7*, 319.
(6) (a) Croce, F.; Curini, R.; Martinelli, A.; Persi, L.; Ronci, F.; Scrosati, B. *J. Phys. Chem. B* **1999**, *103*, 10632. (b) Croce, F.; Persi, L.; Scrosati, B.; Serraino-Fiory, F.; Plichta, E.; Hendrickson, M. A. *Electrochim. Acta* **2001**, *46*, 2457. (c) Scrosati, B.; Croce, F.; Persi, L. *J. Electrochem. Soc.* **2000**, *147*, 1718. (d) Croce, F.; Persi, L.; Ronci, F.; Scrosati, B. *Solid State Ionics* **2000**, *135*, 47. (e) Appetecchi, G. B.; Croce, F.; Dautzenberg, G.; Mastragostino, M.; Ronci, F.; Scrosati, B.; Soavi, F.; Zanelli, A.; Alessandrini, F.; Prosini, P. P. *J. Electrochem. Soc.* **1998**, *145*, 4126.
(7) (a) Byrne, N.; Efthimiadis, J.; MacFarlane, D. R.; Forsyth, M. *J. Mater. Chem.* **2004**, *14*, 127. (b) Wang, M. K.; Zhao, F.; Dong, S. J. *J. Phys. Chem. B* **2004**, *108*, 1365. (c) Walls, H. J.; Riley, M. W.; Singhal, R. R.; Spontak, R. J.; Fedkiw, P. S.; Khan, S. A. *Adv. Funct. Mater.* **2003**, *13*, 710. (d) Singhal, R. G.; Capracotta, M. D.; Martin, J. D.; Khan, S. A.; Fedkiw, P. S. *J. Power Sources* **2004**, *128*, 247. (e) Choi, N. S.; Lee, Y. M.; Lee, B. H.; Lee, J. A.; Park, J. K. *Solid State Ionics* **2004**, *167*, 293.
(8) Baerlocher, C.; Meier, W. M.; Olson, D. H. *Atlas of Zeolite Framework Types,* 5th ed.; Elsevier: Amsterdam, 2001.
(9) (a) Corma, A. *Chem. Rev.* **1997**, *97*, 2373. (b) Cundy, C. S.; Cox, P. A. *Chem. Rev.* **2003**, *103*, 663.
(10) Xi, J. Y.; Ma, X. M.; Cui, M. Z.; Huang, X. B.; Zheng, Z.; Tang, X. Z. *Chin. Sci. Bull.* **2004**, *49*, 785.
(11) Broyer, M.; Valange, S.; Bellat, J. P.; Bertrand, O.; Weber, G.; Gabelica, Z. *Langmuir* **2002**, *18*, 5083.
(12) Newalkar, B. L.; Choudary, N. V.; Turaga, U. T.; Vijayalakshmi, R. P.; Kumar, P.; Komarneni S.; Bhat, T. S. G. *Micropor. Mesopor. Mater.* **2003**, *65*, 267.
(13) (a) Zhao, D. Y.; Feng, J. L.; Huo, Q. S.; Melosh, N.; Fredrickson, G. H.; Chmelka, B. F.; Stucky, G. D. *Science* **1998**, *279*, 548. (b) Zhao, D. Y.; Huo, Q. S.; Feng, J. L.; Chmelka, B. F.; Stucky, G. D. *J. Am. Chem. Soc.* **1998**, *120*, 6024. (c) Che, S. N.; Lund, K.; Tatsumi, T.; Iijima, S.; Joo, S. H.; Ryoo, R.; Terasaki, O. *Angew. Chem., Int. Ed.* **2003**, *42*, 2182.
(14) (a) Pietrogiacomi, D.; Campa, M. C.; Tuti, S.; Indovina, V. *Appl. Catal., B* **2003**, *41*, 301. (b) Yadav, G. D.; Sengupta, S. *Org. Process Res. Dev.* **2002**, *6*, 256. (c) Mishra, H. M.; Parida, K. M. *Appl. Catal., A* **2002**, *224*, 179. (d) Ecormier, M. A.; Wilson, K.; Lee, A. F. *J. Catal.* **2003**, *215*, 57. (e) Xi, J. Y.; Tang, X. Z. *Chem. Phys. Lett.* **2004**, *393*, 271.
(15) (a) Bruce, P. G.; Vincent, C. A. *J. Electroanal. Chem.* **1987**, *225*, 1. (b) Evans, J.; Vincent, C. A.; Bruce, P. G. *Polymer* **1987**, *28*, 2324. (c) Riley, M.; Fedkiw, P. S.; Khan, S. A. *J. Electrochem. Soc.* **2002**, *149*, A667.
(16) (a) Wells, D. H.; Delgass, W. N.; Thomson, K. T. *J. Am. Chem. Soc.* **2004**, *126*, 2956. (b) Zhuang, J. Q.; Ma, D.; Yan, Z. M.; Deng, F.; Liu, X. M.; Han, X. W.; Bao, X. H.; Liu, X. W.; Guo, X. W.; Wang, X. S. *J. Catal.* **2004**, *221*, 670.
(17) (a) Vaia, R. A.; Vasudevan, S.; Krawiec, W.; Scanlon, L. G.; Giannelis, E. P. *Adv. Mater.* **1995**, *7*, 154. (b) Fan, L. Z.; Nan, C. W.; Li, M. *Chem. Phys. Lett.* **2003**, *369*, 698. (c) Sandí, G.; Carrado, K. A.; Joachin, H.; Lu, W. Q. Prakash, J. *J. Power Sources* **2003**, *119*−*121*, 492.
(18) (a) Salomon, M.; Xu, M.; Eyring, E. M.; Petrucci, S. *J. Phys. Chem.* **1994**, *98*, 8234. (b) Wieczorek, W.; Zalewska, A.; Raducha, D.; Florjanczyk, Z.; Stevens, J. R. *J. Phys. Chem. B* **1998**, *102*, 352. (c) Wieczorek, W.; Raducha, D.; Zalewska, A.; Stevens, J. R. *J. Phys. Chem. B* **1998**, *102*, 8725.

MA048849D